



Cite this: *Chem. Commun.*, 2025, **61**, 13841

## Peptide self-assembly meets photodynamic therapy: from molecular design to antitumor applications

Shukun Li, <sup>ab</sup> Jan C. M. van Hest, <sup>b</sup> Ruirui Xing <sup>\*ac</sup> and Xuehai Yan <sup>\*ac</sup>

Peptide-based photosensitive nanodrugs have emerged as a versatile and programmable nanoplatform for photodynamic therapy (PDT). By harnessing the inherent biocompatibility, structural programmability, and functional tunability of peptide in combination with the photoactivity of photosensitizer (PS), these supramolecular assemblies offer precise control over the photophysical properties and tumoral delivery of PS. In this review, we highlight recent advances in the design and engineering of peptide–PS nanodrugs, with a focus on the underlying noncovalent interactions, structural design principles, and functional integration. We further discuss how these supramolecular nanodrugs effectively overcome key barriers in tumoral delivery for PDT. Finally, we provide a perspective on the current challenges and future opportunities for translating peptide-based photosensitive nanodrugs into clinical practice.

Received 15th July 2025,  
 Accepted 12th August 2025

DOI: 10.1039/d5cc03988f

[rsc.li/chemcomm](http://rsc.li/chemcomm)

### 1. Introduction

Photodynamic therapy (PDT) is an antitumor therapeutic modality that relies on the selective accumulation of photosensitizer (PS) at the lesion site, followed by light irradiation to

activate the PS and trigger the generation of cytotoxic reactive oxygen species (ROS), ultimately inducing tumor cell death.<sup>1</sup> This approach offers several clinical advantages, including high spatial precision, minimal invasiveness, and low systemic toxicity.<sup>2</sup> Since its first reported clinical application in 1976,<sup>3</sup> where hematoporphyrin was administered to five bladder cancer patients and tumor growth inhibition was observed in one case, PDT has attracted considerable attention as a promising oncological strategy. However, despite its early promise, the broader clinical translation of PDT has been hindered by the intrinsic limitations of conventional PS molecules.<sup>4</sup> Most PS molecules are inherently hydrophobic, which results in poor

<sup>a</sup> State Key Laboratory of Biopharmaceutical Preparation and Delivery, Institute of Process Engineering, Beijing 100190, China. E-mail: rrxing@ipe.ac.cn, yanxh@ipe.ac.cn; Web: <https://www.yan-assembly.org/>

<sup>b</sup> Bio-Organic Chemistry, Institute for Complex Molecular Systems, Eindhoven University of Technology, P.O. Box 513, 5600 MB Eindhoven, The Netherlands

<sup>c</sup> School of Chemical Engineering, University of Chinese Academy of Sciences, Beijing 100049, China



**Shukun Li**

*Shukun Li received her PhD degree from IPE, CAS in 2021 with Prof. Yan. She then was supported by the International Postdoctoral Exchange Fellowship Program to start her postdoctoral research in IPE and TU/e. In 2023, she became the Marie Skłodowska-Curie Postdoctoral Fellow and continued the research in TU/e. Her research interests are focused on polymer- or peptide-modulated self-assemblies and their applications in tumor immunotherapy.*



**Jan C. M. van Hest**

*Jan C. M. van Hest obtained his PhD from TU/e in 1996 with Prof. E. W. Meijer. In 2000, he was appointed full professor at Radboud University Nijmegen. As of September 2016, he holds the chair of Bio-Organic Chemistry at TU/e. Since May 2017, he is the scientific director of the ICMS. The group's focus is to develop well-defined compartments for nanomedicine and artificial cell research, using a combination of techniques from polymer science to protein engineering.*



aqueous solubility, uncontrolled aggregation under physiological conditions, and reduced photoactivity due to self-quenching effects. In addition, free PS molecules often exhibit suboptimal pharmacokinetics and biodistribution, lacking sufficient tumor accumulation, controlled release and deep penetration.<sup>5</sup> These drawbacks collectively diminish their therapeutic efficacy *in vivo* and pose significant challenges for clinical implementation. These limitations collectively compromise their therapeutic efficacy *in vivo* and complicate their clinical implementation worldwide.

Peptide self-assembly has emerged as a powerful bottom-up strategy for the construction of supramolecular nanodrugs, offering inherent advantages such as excellent biocompatibility, structural programmability, and facile integration of functional motifs.<sup>6–8</sup> Driven by a variety of noncovalent interactions, including  $\pi$ - $\pi$  stacking, hydrogen bonding, hydrophobic effects, electrostatic forces, and metal coordination, peptide-based supramolecular systems can organize into well-defined nanostructures capable of encapsulating, stabilizing, or co-assembling with functional molecules.<sup>9–11</sup> With the convergence of peptide self-assembly and PDT, new possibilities have emerged to address the longstanding limitations of conventional PS molecules. By incorporating PS into these peptide-based architectures, researchers have achieved significant improvements in their physicochemical and biological behaviors. These include enhanced aqueous solubility, preservation of photophysical properties, and the introduction of multifunctional capabilities such as tumor targeting, stimuli-responsive behavior, and improved tumoral accumulation.<sup>12–15</sup>

In our own research efforts, we have systematically investigated a broad spectrum of peptide-based photosensitive nanodrugs to optimize the assembly, delivery, and functional performance of PS in the context of PDT. In this review, we provide a comprehensive overview of recent advances in this field. We begin by introducing the underlying noncovalent interactions and design principles that govern the self-assembly of peptides and photosensitizers. This is followed by a discussion of key strategies employed to engineer photosensitive nanodrugs with tailored functionalities. We then highlight how these nanodrugs enhance the tumoral



Fig. 1 Schematic illustration of peptide-based photosensitive nanodrugs, highlighting their construction through noncovalent interactions, self-assembly strategies, tumor delivery behaviors, and versatility in combination therapy.

delivery and therapeutic performance of PS. Representative examples of PDT, both as a standalone modality and in combination with other therapies, are provided to demonstrate their improved therapeutic efficacy as well (Fig. 1). Finally, we outline the current challenges and future opportunities that will shape the development and clinical translation of peptide-based photosensitive nanodrugs.

## 2. Assembly mechanism

### 2.1 Assembly interactions

Noncovalent interactions, including  $\pi$ - $\pi$  stacking, hydrogen bonding, hydrophobic effect, electrostatic force, and metal coordination, play a central role in directing the organization



Ruirui Xing

Ruirui Xing is currently an associate professor at IPE, CAS. Her research interests are focused on the design and self-assembly of functional peptides, supramolecular effects, nanomaterials and nanodrugs, and applications in the field of biomedicine.



Xuehai Yan

Xuehai Yan is a full professor at the IPE, CAS. Currently, he serves as the Deputy Director of the IPE, CAS, and as an Associate Editor of ACS Applied Materials and Interfaces. His research focuses on peptide self-assembly and engineering, liquid-liquid phase separation, biomolecular condensates and noncovalent glass, supramolecular colloids and crystals, as well as their applications in antimicrobial, anti-inflammatory, and anticancer therapies.



of peptide and PS into well-defined photosensitive nanodrugs.<sup>16</sup> The intrinsic programmability of peptides, achieved by the precise combination of amino acid residues, enables fine-tuning of these interactions while also allowing the incorporation of functional moieties, such as stimuli-responsive units or targeting ligands, either from the amino acids themselves or through conjugation with other molecules.<sup>17</sup> This versatility significantly enhances the structural and functional flexibility of these nanodrugs. More importantly, compared to covalent bonds, noncovalent interactions possess relatively lower activation energies ( $E_a$ ), allowing the nanodrugs to dynamically respond to specific environmental stimuli.<sup>18</sup> This dynamic and reversible nature is crucial for achieving controlled release and environment-adaptive behavior in therapeutic contexts.

## 2.2 Assembly strategy

Based on our group's research efforts, we categorize four main strategies to facilitate the formation of peptide-PS nanodrugs: (i) co-assembly of peptide and PS; (ii) self-assembly of chemically tethered peptide-PS conjugate; (iii) interface-directed assembly and (iv) covalent-crosslinked assembly of peptide and PS.

**2.2.1 Co-assembly of peptide and PS.** Considering PS as the integral building block equipped with noncovalent interactional groups, peptide often act as the modulator that guide the assembly process into well-defined nanostructures. For example,<sup>19</sup> amphiphilic dipeptides such as H-Phe-Phe-NH<sub>2</sub>-HCl (CDP) or fluorenylmethoxycarbonyl (Fmoc)-protected amino acids like Fmoc-L-Lys can co-assemble with the hydrophobic PS chlorin e6 (Ce6). This co-assembly is primarily driven by hydrophobic interactions and  $\pi$ - $\pi$  stacking between the Fmoc groups or aromatic residues in peptides and the pyrrole

rings of Ce6, resulting in the formation of photosensitive nanoparticles (NPs). This design principle can be extended to other small-molecule modulators as well. For instance,<sup>20</sup> adenosine triphosphate (ATP), carrying multiple negative charges, enables cationic porphyrin monomers to co-assemble into photosensitive superhelical nanofibers through electrostatic and other noncovalent interactions in aqueous solution.

Moreover, bioinspired metallo-nanodrugs have been developed by mimicking hemoglobin-like coordination (Fig. 2(A)).<sup>21</sup> Metal-binding peptides, such as Fmoc-L-histidine (Fmoc-H) and *N*-benzyloxycarbonyl-L-histidine-L-phenylalanine (Z-HF), serve as assembly units. Zinc ions ( $Zn^{2+}$ ) facilitate dual coordination: with histidine residues *via* imidazole- $Zn^{2+}$  interactions, and with Ce6 *via* its chlorin ring. These interactions, along with hydrophobic and  $\pi$ - $\pi$  stacking between the peptide and Ce6 moieties, drive the formation of spherical metallo-nanodrugs, with average sizes of 79 nm and 76 nm for Fmoc-H/ $Zn^{2+}$ /Ce6 and Z-HF/ $Zn^{2+}$ /Ce6, respectively (Fig. 2(B) and (C)). Notably, such coordination bonds exhibit dual characteristics, providing structural stability under physiological conditions, while enabling stimulus-responsive disassembly in the tumor micro-environment (TME) due to acidic pH and elevated glutathione (GSH) levels, which promote carboxyl protonation and competitive  $Zn^{2+}$  chelation. Together, these examples illustrate the versatility of co-assembly strategies in constructing functional peptide-PS nanostructures through finely tuned noncovalent interactions.

**2.2.2 Self-assembly of chemically tethered peptide-PS conjugate.** Peptide containing self-assembling motif can be chemically tethered to PS to form unified conjugated building block. This covalent linkage not only preserves the individual functionalities of both components but also enhances



**Fig. 2** Assembly strategy. (A) Schematic illustration of the fabrication of metallo-nanodrugs *via*  $Zn^{2+}$ -coordinated self-assembly with small peptides and photosensitizers. TEM images of (B) Fmoc-H/ $Zn^{2+}$ /Ce6 and (C) Z-HF/ $Zn^{2+}$ /Ce6. Adapted from ref. 21, with permission from 2018 American Chemical Society. (D) Schematic illustration of self-assembly of phthalocyanine-peptide conjugates. (E) DLS result and (F) TEM image of PF NPs. Adapted from ref. 23, with permission from 2019 Wiley-VCH Verlag GmbH & Co. KGaA, Weinheim.



intermolecular interactions, offering greater control over the resulting nanostructures.<sup>22</sup> For instance,<sup>23</sup> our group synthesized phthalocyanine–diphenylalanine conjugate (ZnPc-FF, PF) as modular building block. These PFs undergo self-assembly into well-defined PF NPs, driven by strong hydrophobic interactions and  $\pi$ - $\pi$  stacking (Fig. 2(D)). The resulting nanodrugs showed an average diameter of 55 nm (Fig. 2(E)), spherical morphology (Fig. 2(F)), and exhibited excellent colloidal stability and enhanced supramolecular photothermal properties. Of note, the strengthened intermolecular interactions in PF NPs facilitate charge or energy transfer, leading to complete fluorescence quenching and suppression of intersystem crossing (ISC), thereby favoring photothermal conversion.<sup>24</sup> However, upon interaction with hydrophobic cell membranes, the PF NPs disassemble, triggering an adaptive shift from a photothermal to a photodynamic response. In addition, this peptide–PS conjugation strategy provides the versatility to integrate diverse therapeutic modalities. For example,<sup>25</sup> conjugating peptide nucleic acids (PNAs) with porphyrin or boron–dipyrromethene (BODIPY) results in PNA–porphyrin and PNA–BODIPY (PNA–BDP) conjugates, which self-assemble into photodynamically active nanoparticles. Overall, covalent peptide–PS conjugates represent a powerful strategy to enhance assembly fidelity, modulate functional outcomes, and enable multi-modal therapeutic design.

**2.2.3 Interface-directed assembly.** Interface-directed assembly has proven effective in suppressing the Ostwald ripening of hydrophobic drug molecules.<sup>26</sup> For example, naturally occurring polyphenols such as tannin (TA) can coordinate with  $\text{Fe}^{3+}$  ions to form TA– $\text{Fe}^{3+}$  complexes, which spontaneously assemble into thin films or coatings.<sup>27</sup> This strategy has been successfully applied to hydrophobic drugs like paclitaxel (PTX), where the TA– $\text{Fe}^{3+}$  coating on PTX cores prevents further particle growth, thereby ensuring long-term colloidal stability. Building on this principle, our group demonstrated its versatility for hydrophobic PS (Fig. 3(A)).<sup>28</sup>

Ce6 was first dissolved in alkaline solution to obtain its ionic form. Upon pH reduction, Ce6 aggregated to form an opalescent suspension. Subsequent addition of TA and  $\text{FeCl}_3$  led to the formation of an interfacial TA– $\text{Fe}^{3+}$  coating, resulting in Ce6@TA– $\text{Fe}^{3+}$  NPs approximately 60 nm in diameter (Fig. 3(B) and (C)). Compared to free Ce6 without interfacial assembly, Ce6@TA– $\text{Fe}^{3+}$  NPs showed significantly improved tumor-targeted accumulation and a markedly enhanced photodynamic therapeutic effect. Overall, interfacial self-assembly offers a universal and efficient strategy to stabilize hydrophobic PS while enhancing their biological performance *in vivo*.

**2.2.4 Covalent-crosslinked assembly.** Covalently triggered peptide self-assembly is achieved through the sequential integration of spontaneous covalent reactions and noncovalent interactions, thereby enhancing the physiological stability and expanding the functional versatility of the resulting peptide-based nanodrugs.<sup>29</sup> A representative example is the Schiff base reaction, in which aldehyde (or ketone) groups react with amine groups to form imine bonds ( $-\text{C}=\text{N}-$ ), generating only water as a byproduct, an ideal condition for biomedical applications.<sup>30</sup> In our group, we demonstrated that this reaction can serve as a crosslinking mechanism to reinforce nanoparticle stability.<sup>31</sup> Specifically, glutaraldehyde (GA), a commonly used biomedical crosslinker, facilitated the assembly of the dipeptide CDP while simultaneously encapsulating the hydrophobic photosensitizer Ce6 (Fig. 3(D)). The resulting crosslinked, positively charged CDP/Ce6 NPs were further stabilized through electrostatic interaction with negatively charged heparin (Hep), forming Hep/CDP/Ce6 NPs with an average diameter around 100 nm (Fig. 3(E) and (F)). Compared to free Ce6, the Hep/CDP/Ce6 NPs significantly prolonged blood circulation time and exhibited improved anticancer efficacy *in vivo*. This strategy highlights how covalent chemistry can be leveraged to reinforce peptide nanodrugs and enhance the therapeutic performance of photosensitizers in PDT applications.



**Fig. 3** Assembly strategy. (A) Interface-directed assembly of Ce6-encapsulated TA– $\text{Fe}^{3+}$  nanoparticles. (B) DLS result and (C) TEM image of Ce6@TA– $\text{Fe}^{3+}$  NPs. Adapted from ref. 28, with permission from 2017, The Author(s). (D) Covalent crosslinked assembly of dipeptides and glutaraldehyde, with Ce6 encapsulation and heparin surface modification. (E) DLS result and (F) TEM image of Hep/CDP/Ce6 NPs. Adapted from ref. 31, with permission from 2016, American Chemical Society.



Table 1 Comparative summary of assembly strategies

Assembly strategy	Advantages	Limitations
Co-assembly of peptide and PS	Simple preparation High loading capacity Tunable nanostructures	Relatively lower structural stability Limited control over PS distribution
Self-assembly of chemically tethered peptide-PS conjugate	Enhanced structural stability Precise stoichiometric control Well-defined nanostructures	Synthetic complexity Limited drug loading if only one PS per conjugate
Interface-directed assembly	Enhanced encapsulation stability Fine control over surface modification	Complex fabrication procedures Limited scalability for large-scale production
Covalent-crosslinked assembly	Excellent stability Expanded functional diversity	Uncontrolled side reactions during chemical crosslinking Possible reduced biocompatibility due to crosslinkers Limited scalability for large-scale production

Table 1 provides a comparative overview of four representative assembly strategies for PDT, highlighting their respective advantages and limitations. Co-assembly of peptide and PS offers simplicity, high PS loading, and tunable nanostructures, but may suffer from reduced structural stability and limited control over component distribution. Self-assembly of chemically tethered peptide-PS conjugate enables precise molecular design and improved nanostructure definition, though it may be synthetically demanding and restricted in drug loading capacity. Interface-directed assembly allows for enhanced encapsulation stability and surface engineering but often involves complex fabrication steps and faces scalability challenges. Nanodrugs formed *via* covalent-crosslinked assembly offer excellent stability and enhanced functional versatility; however, potential biocompatibility concerns and crosslinking side reactions may hinder their translational potential. Understanding the trade-offs between these strategies is essential for rational design and application of peptide-based photosensitive nanodrugs in pre-clinical and clinical settings.

### 2.3 Roles of peptides in nanodrugs

The photophysical performance of PS, such as absorption, fluorescence, and ROS generation, is closely influenced by their surrounding microenvironment. Peptide-based self-assembly provides a versatile strategy to modulate these properties through structural organization and intermolecular interactions.

During peptide assembly, densely packed PS molecules often undergo  $\pi$ - $\pi$  stacking and hydrophobic interactions. While such close proximity can promote self-aggregation and self-quenching, leading to reduced fluorescence and diminished ROS production. Rational design strategies have been developed to mitigate these effects. For instance, doping porphyrins into peptide-based nanoparticles spatially separates the PS molecules, preserving their intrinsic fluorescence, minimizing dose-related side effects, and enabling efficient two-photon photodynamic activity.<sup>32</sup> Moreover, the supramolecular architecture of peptide assemblies can protect PS from photodegradation, enhancing their photostability under physiological conditions. As demonstrated by peptide-indocyanine nanodrugs,<sup>33</sup> such constructs retain the optical properties of

indocyanines while shielding them from degradation, ensuring sustained therapeutic availability during treatment.

Overall, peptide-guided assembly not only enables precise structural control but also provides a powerful means to fine-tune the photophysical behavior of PS. Additionally, peptides offer exceptional programmability, allowing the incorporation of functional motifs such as tumor-targeting ligands, stimuli-responsive groups, and biological regulators. These features collectively support the rational design of nanodrugs with enhanced tumoral delivery, as further discussed in Section 3.

## 3. Tumoral delivery behaviors

To fully realize the therapeutic potential of peptide-based photosensitive nanodrugs, it is essential to address key challenges associated with tumoral delivery. Rational design strategies have been developed to optimize pharmacokinetics and targeting, enable stimuli-responsive release, and enhance tumor penetration and retention. In the following sections, we present representative examples to highlight recent advances in each of these three areas.

### 3.1 Pharmacokinetics optimization and targeted delivery

To ensure sufficient accumulation of PS at the tumor site, enhancing the stability of photosensitive nanodrugs to optimize their pharmacokinetics represents a promising strategy. In our research, we developed a metal-coordination-driven co-assembly approach to improve the structural stability of peptide-based photosensitive nanosystems and demonstrated improved pharmacokinetic profiles. For example,<sup>34</sup> we co-assembled a histidine-containing peptide with biliverdin through noncovalent interactions to form ZB NPs. To further stabilize the structure,  $Mn^{2+}$  ions were introduced, resulting in the formation of ZBMn NPs (Fig. 4(A)). Compared to the uncoordinated ZB NPs, ZBMn NPs exhibited prolonged blood circulation half-life and more favorable pharmacokinetics, particularly during the initial distribution phase (Fig. 4(B)). Biodistribution studies revealed that both ZB and ZBMn NPs reached peak tumor accumulation approximately 6 hours post-injection, with ZBMn NPs displaying superior tumor uptake



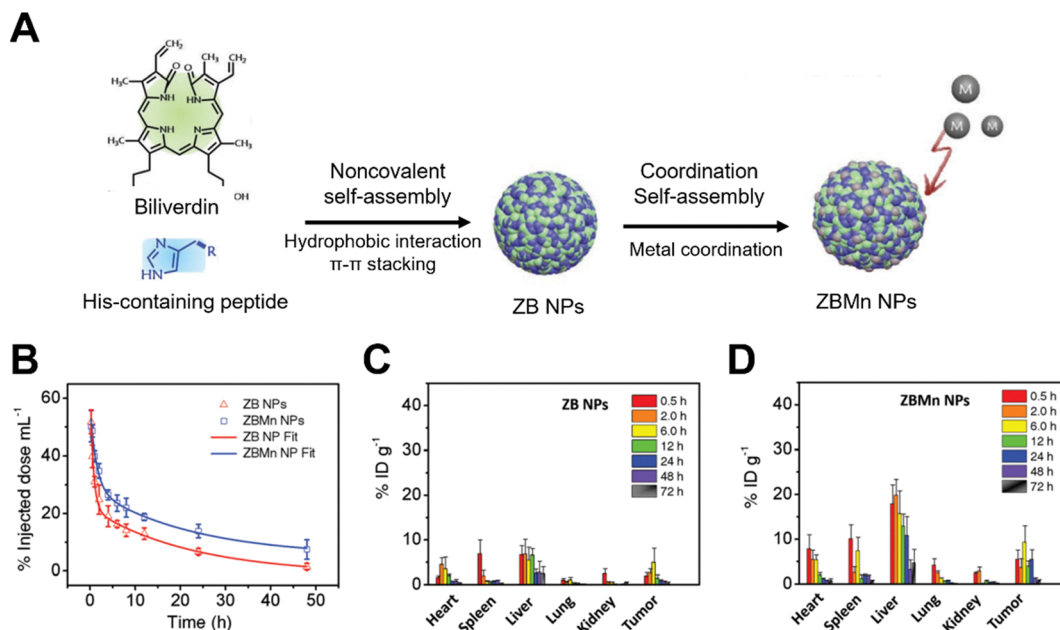


Fig. 4 Pharmacokinetic optimization to enhance PS accumulation at the tumor site. (A) Schematic illustration of the fabrication of ZB NPs and ZBMn NPs. (B) Blood elimination kinetics of the ZB NPs and ZBMn NPs. Biodistribution of the (C) ZB NPs and (D) ZBMn NPs. Adapted from ref. 34, with permission from 2019 Wiley-VCH Verlag GmbH & Co. KGaA, Weinheim.

due to their enhanced circulation time (Fig. 4(C) and (D)). In another example,<sup>35</sup> we utilized the metal-binding protein ovalbumin (OVA), zinc ions ( $Zn^{2+}$ ), and the photosensitizer pheophorbide A (PheoA) to construct a supramolecular photosensitive nanodrug. The resulting nanodrug exhibited excellent colloidal stability under dilution and in physiologically relevant media, while also demonstrating selective accumulation at the tumor site *in vivo*.

Incorporating active targeting mechanisms provides an additional approach to improve drug delivery efficiency and tumor specificity. Targeting motifs such as receptor-specific peptides (*e.g.*, RGD for integrin receptors<sup>36</sup>) or small-molecule ligands (*e.g.*, folic acid for folate receptors<sup>37</sup>) can be tethered to peptide building blocks. The resulting nanodrugs would promote ligand–receptor recognition on tumor cell surfaces. Moreover, subcellular targeting can be achieved through the introduction of organelle-specific moieties. For instance,<sup>38</sup> the incorporation of positively charged pyridinium groups into the nanodrug system facilitates preferential mitochondrial localization, thereby enhancing therapeutic outcomes. Alternatively, peptides can be rationally designed to function as cell-penetrating peptides (CPPs), such as the well-known sequences TAT (YGRKKRRQRRR) or penetratin (RQIKIWFQNRRMKWKK), which improve cellular uptake and transmembrane transport.<sup>39</sup> Overall, these strategies collectively help ensure an effective PS dose reaches the tumor tissue.

### 3.2 TME-responsive release

Site-specific drug release through stimuli-responsive mechanisms characteristic of the TME offers a promising strategy to enhance therapeutic efficacy while minimizing systemic toxicity.

Key features of the TME, such as acidic pH, elevated GSH levels, and the overexpression of tumor-specific enzymes (*e.g.*, MMP-2 and cathepsin B), have been widely exploited for triggered drug release.<sup>40</sup> For example,<sup>41</sup> a photosensitive nanodrug was developed *via* electrostatic assembly between negatively charged proteins and positively charged polylysine (PLL), stabilized by intermolecular disulfide crosslinking and surface PEGylation. This system was capable of encapsulating various PS molecules, including Ce6, protoporphyrin IX (PpIX), and verteporfin (Fig. 5(A)). The resulting Ce6-NPs exhibited multiple stimuli-responsiveness, releasing their payload rapidly in response to acidic pH, reductive conditions (high GSH), and elevated protease concentrations, effectively mimicking the TME (Fig. 5(B) and (C)). *In vivo* studies confirmed the rapid Ce6 release within tumor tissues and demonstrated effective tumor ablation under light irradiation.

In another study,<sup>42</sup> we constructed a photosensitive nanoparticle system by electrostatically assembling hyaluronic acid (HA) and PLL. *In situ* disulfide crosslinking facilitated stable nanoparticle formation, enabling efficient Ce6 encapsulation. These nanoparticles also have been demonstrated synergistic responsiveness to both acidic pH and elevated GSH concentrations, thereby enhancing Ce6 release and PDT performance. Together, these examples highlight how rational design of TME-responsive supramolecular nanodrugs enables precise, on-demand release of PS in tumors, ultimately improving therapeutic selectivity and photodynamic efficacy.

### 3.3 Enhanced tumor retention and penetration

Improving deep tissue penetration and long-term retention of nanodrugs within tumor tissues is a critical strategy to



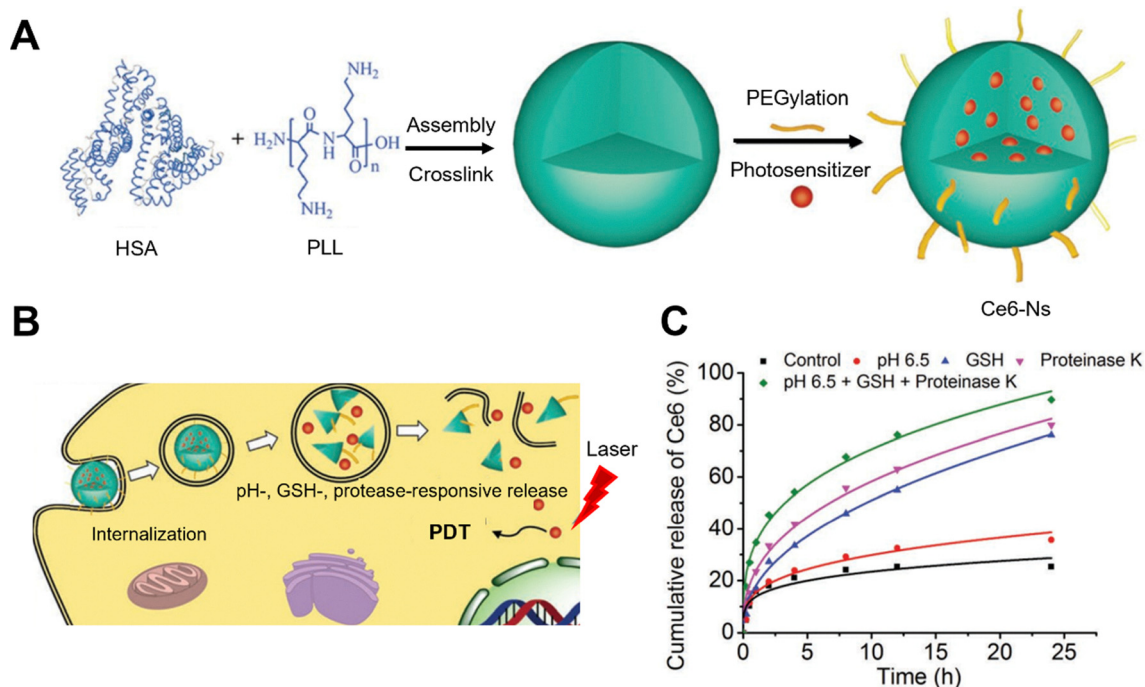


**Fig. 5** TME-responsive release to enhance therapeutic efficacy. (A) Schematic illustration of the fabrication of Ce6-loaded nanoparticles, Ce6-Ns. (B) Schematic depiction of the stimuli-responsive release of Ce6 from Ce6-Ns. (C) Release profiles of Ce6 under different conditions, including variations in pH, GSH, and protease levels. Adapted from ref. 41, with permission from 2016 Wiley-VCH Verlag GmbH & Co. KGaA, Weinheim.

overcome biological barriers such as limited diffusion and rapid systemic clearance, thereby enhancing therapeutic outcomes.

Stimuli-responsive structural transformation has emerged as a promising approach to address these challenges by enabling dynamic modulation of nanoparticle behavior within the TME.<sup>43</sup> For instance,<sup>44</sup> a peptide-porphyrin conjugate (PWG) was constructed by coupling a pH-responsive dipeptide tryptophan-glycine (WG) to a hydrophobic porphyrin core *via* amidation. PWG self-assembled into nanoparticles under physiological conditions but underwent protonation-induced transformation into nanofibers in the acidic TME (Fig. 6(A)). This transition was driven by enhanced intermolecular hydrogen bonding, resulting in significantly prolonged retention (up to 360 hours post-injection hours, Fig. 6(B)–(D)) and enhanced singlet oxygen generation, both essential for effective PDT.

In another example,<sup>45</sup> co-assembled nanoparticles were designed using elastin-like polypeptides (ELPs) with a temperature-sensitive diblock structure ([A3G2-60]-[V4F1-50]) and a PS-conjugated ELP (TT1-[M1V3-40]). Phenylalanine residues in the hydrophobic core provided  $\pi$ - $\pi$  interactions with the PS, stabilizing the nanoparticle structure. To improve tumor targeting, an anti-EGFR nanobody (7D12) was genetically fused to the ELP, enhancing selective uptake by EGFR-overexpressing cancer cells. Upon light-triggered photooxidation, the hydrophobic PS-conjugated segments became hydrophilic, inducing nanoparticle disassembly. However,  $\pi$ - $\pi$  interactions between phenylalanine and the PS drove the re-formation of smaller nanoparticles. These transformed particles showed deeper tumor penetration and more efficient cell killing, thanks to their reduced size and preserved targeting capability.

Supramolecular hydrogels offer a compelling formulation strategy for enhancing drug retention at tumor sites by functioning as localized drug depots with sustained release profiles. For instance,<sup>46</sup> bola-dipeptide-based hydrogels (using a di-FF derivative, DFF) self-assemble into fibrous networks in aqueous environments, forming stable, biocompatible, and injectable systems. These hydrogels efficiently encapsulate the photodynamic prodrug 5-aminolevulinic acid hydrochloride (5-ALA), enabling its localized delivery and *in situ* conversion to the active photosensitizer PpIX. This strategy minimizes off-target leakage, promotes site-specific activation, and achieves durable tumor inhibition. In another example,<sup>47</sup> injectable hydrogels formed from Fmoc-FF and PLL were utilized to deliver Ce6. These hydrogels, featuring shear-thinning and self-healing properties, are ideal for local administration. They enable sustained Ce6 release and support multiple rounds of photodynamic therapy after a single injection, effectively suppressing tumor growth with minimal systemic toxicity.

## 4. Applications

Building on the aforementioned construction strategies and biological behavior modulation, diverse therapeutic modalities of PDT have been developed and explored.

### 4.1 Imaging-guided PDT

A supramolecular nanotheranostic based on fluorescence imaging-guided PDT was constructed through the Fmoc-L-leucine (Fmoc-L-L)-mediated self-assembly of Mn<sup>2+</sup> ions and the photosensitizer Ce6. The coordination interaction facilitated the





**Fig. 6** Stimuli-responsive structural transformation to enhanced PS retention within tumor. (A) Schematic of PWG nanoparticle self-assembly, acid-triggered transformation, and application in PDT. (B) Fluorescence images of tumor-bearing mice over 192 h after intravenous injection of PWG NPs. (C) Quantified tumor fluorescence intensity corresponding to (B). (D) *Ex vivo* fluorescence images of major organs at 24, 72, and 360 h post-injection. Adapted from ref. 44, with permission from 2020 The Authors. Published by Wiley-VCH GmbH.

co-assembly of Fmoc-L-L and  $Mn^{2+}$  into nanostructures, which could adaptively encapsulate Ce6. The resulting nanodrug exhibited high drug-loading capacity, excellent biocompatibility, and strong stability, while being responsive to intracellular GSH, triggering smart disassembly. Notably,  $Mn^{2+}$  played a dual role: enabling magnetic resonance imaging (MRI) to monitor drug delivery and enhancing PDT efficacy by scavenging GSH, thus improving the oxidative microenvironment. This system successfully demonstrated imaging-guided PDT with improved therapeutic outcomes.<sup>48</sup>

#### 4.2 Combination of photothermal therapy and PDT

An injectable collagen-gold hybrid hydrogel was developed using a biomineralization-triggered process, where positively charged collagen chains electrostatically interacted with  $[AuCl_4]^-$  ions to form *in situ* gold nanoparticles (AuNPs) as crosslinkers. The resulting hydrogels exhibited shear-thinning and self-healing properties, biodegradability, and photothermal activity due to embedded AuNPs. After encapsulating the photosensitizer TMPyP, the hybrid hydrogel enabled combined photothermal and photodynamic therapy. Localized intratumoral injection provided sustained release and spatial confinement of therapeutic agents, enabling efficient synergistic treatment with minimized systemic toxicity.<sup>49</sup>

#### 4.3 Combination of chemotherapy and PDT

Two zinc(II) phthalocyanine (ZnPc)-peptide conjugates, ZnPc-GGK(B)-COOH and ZnPc-GGK(B)-CONH<sub>2</sub>, were synthesized and self-assembled into nanoparticles displaying biotin moieties on their surfaces for targeted delivery. The nanoparticles demonstrated differential surface charges and stability depending on the C-terminal modification. ZnPc-GGK(B)-COOH NPs

were selectively taken up by HepG2 cancer cells, which are known to overexpress biotin-specific receptors,<sup>50</sup> thereby facilitating receptor-mediated endocytosis of the biotin-functionalized nanostructures. Co-assembly with doxorubicin (DOX) yielded ZnPc-GGK(B)-COOH/DOX NPs, which exhibited synergistic photodynamic and chemotherapeutic effects, achieving superior tumor inhibition both *in vitro* and *in vivo*, with reduced IC<sub>50</sub> values and enhanced apoptosis.<sup>51</sup>

#### 4.4 Combination of immunotherapy and PDT

pH-responsive porphyrin-peptide nanosheets (PRGD) were constructed by integrating RGD targeting motifs and loaded with the IDO inhibitor NLG919. These nanosheets selectively accumulated in  $\alpha_v\beta_3$  integrin-overexpressing tumor cells and exhibited enhanced singlet oxygen generation under acidic tumor conditions. Upon laser irradiation, the PRGD/NLG919 system not only mediated efficient PDT but also induced robust antitumor immune responses, characterized by increased proliferation of CD3<sup>+</sup>CD8<sup>+</sup> and CD3<sup>+</sup>CD4<sup>+</sup> T cells. This design exemplifies the integration of immunotherapy with PDT for enhanced therapeutic efficacy.<sup>52</sup>

#### 4.5 Combination of TME modulation and PDT

A self-assembled nanodrug was developed using Fmoc-protected cysteine (Fmoc-Cys) and  $Fe^{3+}$  ions, which served both as structural drivers and functional agents. Co-loading with ZnPc photosensitizer and the hypoxia-inducible factor-1 (HIF-1) inhibitor acriflavine (ACF) enabled dual-function nanovesicles (Fmoc-Cys/ $Fe@Pc$ /ACF). Upon cellular internalization,  $Fe^{3+}$  catalyzed H<sub>2</sub>O<sub>2</sub> decomposition to generate O<sub>2</sub>, alleviating hypoxia and enhancing PDT efficiency. The synergistic effect of



ZnPc-mediated phototoxicity and HIF-1 inhibition significantly improved antitumor efficacy in both *in vitro* and *in vivo* models.<sup>53</sup>

## 5. Conclusions

Peptide-based self-assembly systems, owing to their inherent biocompatibility, structural programmability, and multifunctional integration capacity, have emerged as powerful platforms in advancing photodynamic therapy (PDT). These systems provide unique advantages in the realm of precision nanomedicine, enabling the rational design of smart photosensitive nanodrugs.

In this review, we reviewed the underlying assembly mechanisms in Section 2, highlighting the key driving forces and fabrication strategies that enable peptides to function as structural and functional motifs within well-designed supramolecular

architectures. In Section 3, we discussed how these peptide-based systems influence and regulate biological behaviors within the tumor microenvironment, such as pharmacokinetics optimization and targeted delivery, tumor microenvironment-responsive release and enhanced tumor retention and penetration, through rational design strategies. Finally, in Section 4, we demonstrated the versatility of these platforms by presenting representative examples of peptide-based nanodrugs used across various PDT modalities, including imaging-guided therapy, photothermal or chemotherapeutic combinations, immunotherapy, and tumor microenvironment modulation (Table 2).

Despite the substantial progress achieved, several challenges remain to be addressed before clinical translation can be realized. Therefore, we propose the following outlook: (i) molecular engineering of photosensitizer (PS): while nanocarrier systems have substantially improved the solubility, selectivity, and tumor targeting of PS, molecular-level modifications

**Table 2** Summary of representative peptide-based photosensitive nanodrugs for PDT

Building block	Assembly strategy	PS (and others)	Delivery mechanism	Therapeutic outcome	Ref.
<b>Part 2. Assembly mechanism</b>					
H-Phe-Phe-NH <sub>2</sub> -HCl/Fmoc-Lys	Co-assembly	Ce6	Passive targeting	Enhanced photodynamic activity	19
Fmoc-His/Z-His-Phe-OH	Zn <sup>2+</sup> coordination	Ce6	Stimuli-responsive release (pH, GSH)	Improved structural stability and therapeutic effect	21
Phthalocyanine-diphenylalanine conjugate	co-assembly	Phthalocyanine	Cell membrane-triggered photoactivity switch	Photothermal-to-photodynamic conversion	23
PNA-porphyrin/BODIPY conjugate	Self-assembly	Porphyrin	Cell interaction	Enhanced structural stability	25
Tannin-Fe <sup>3+</sup> coating	Self-assembly	BODIPY			
H-Phe-Phe-NH <sub>2</sub> -HCl + glutaraldehyde	Interface-directed assembly	Ce6	Passive targeting	Improved tumor accumulation	28
	Covalent crosslinked assembly	Ce6	Passive targeting	Structural stability and prolonged circulation	31
<b>Part 3. Tumoral delivery behaviors</b>					
Z-His-Obzl	Mn <sup>2+</sup> coordination	Biliverdin	Passive targeting	Enhanced stability and pharmacokinetic profile	34
Ovalbumin	co-assembly	Pheophorbide A	Passive targeting	Colloidal stability and selective tumor uptake	35
HSA + poly-Lys	Zn <sup>2+</sup> coordination			Intelligent and rapid PS release	41
Hyaluronic acid + poly-Lys	Co-assembly & crosslinking	Ce6, PpIX, Verteporfin	TME-responsive (pH, GSH, protease)	Stimuli-responsive PS release	42
Trp-Gly-porphyrin conjugate	Co-assembly & crosslinking	Ce6	TME-responsive-responsive (pH, GSH)		
ELP-anti-EGFR-TT1 conjugate	Self-assembly	Porphyrin	Acid-induced shape transformation	Prolonged tumor retention, enhanced ROS generation	44
Bola-diphenylalanine	Self-assembly	TT1	Temp-triggered nanoparticle shrinkage	Deep tumor penetration, photoactivation	45
Fmoc-FF + poly-Lys	Self-assembly	PpIX	<i>In situ</i> injection	Long-term localized release	46
	Self-assembly	Ce6	<i>In situ</i> injection	Localized sustained release	47
<b>Part 4. Applications</b>					
Fmoc-Leu	Mn <sup>2+</sup> coordination	Ce6	Passive targeting	Improved stability, controlled release	48
Collagen + AuNPs	co-assembly			Combined photothermal therapy and PDT	49
ZnPc-GGK(biotin)-COOH conjugate	Self-assembly & crosslinking	TMPyP	<i>In situ</i> injection		
Porphyrin peptide (PRGD)	Self-assembly	Phthalocyanine + DOX	Receptor-mediated endocytosis	Combined chemotherapy and PDT	51
Fmoc-Cys	Self-assembly	Porphyrin + NLG919	Receptor-mediated endocytosis	Combined immunotherapy and PDT	52
	Fe <sup>3+</sup> coordination	Phthalocyanine	Passive targeting	Combined TME modulation and PDT	53
	co-assembly	Acriflavine			

Abbreviations: PS – photosensitizer; Ce6 – chlorin e6; PpIX – protoporphyrin IX; BODIPY – boron-dipyrromethene; PNA – peptide nucleic acid; DOX – doxorubicin; TME – tumor microenvironment; AuNPs – gold nanoparticles; HA – hyaluronic acid; EGFR – epidermal growth factor receptor; ROS – reactive oxygen species.



remain equally important. For instance, extending the absorbance wavelength of PS through chemical conjugation (*e.g.*, with electron-donating or -withdrawing groups) could overcome the current limitations of light penetration in tissues. This strategy is crucial to unlock the therapeutic potential of PDT for deep-seated tumors; (ii) scalability, manufacturing and clinical translation: the transition from laboratory to clinic demands scalable, reproducible, and cost-effective synthesis. Modular and standardized peptide synthesis strategies, particularly those amenable to solid-phase or automated synthesis, can facilitate large-scale production without compromising structural fidelity or bioactivity. In parallel, clinical translation requires addressing key regulatory and safety concerns, including the biocompatibility and potential immunogenicity of peptide carriers, the toxicity and clearance of their degradation products, and the long-term biosafety of repeated administration. These challenges can be mitigated through the rational design of peptides using endogenous amino acid sequences, the incorporation of biodegradable linkages to promote safe metabolic clearance, and comprehensive immunotoxicological assessments in preclinical models. Furthermore, regulatory frameworks necessitate standardized protocols for characterizing nanostructure morphology, *in vivo* behavior, and pharmacokinetics. Early engagement with regulatory agencies, coupled with strict adherence to good manufacturing practices (GMP) and systematic safety evaluations, will be critical for streamlining clinical development and facilitating regulatory approval; (iii) integration with emerging modalities: peptide-based PDT platforms can be further enhanced through integration with cutting-edge technologies such as immunoengineering and artificial intelligence (AI)-guided drug delivery, enabling personalized treatments and improved therapeutic outcomes. For instance, AI algorithms including computational peptide design tools such as AlphaFold and machine learning-based sequence-structure prediction models can be employed to identify optimal peptide sequences for enhanced self-assembly, efficient photosensitizer encapsulation, and deep tumor penetration. Moreover, AI-driven modeling of tumor-immune microenvironment interactions can support the design of patient-specific therapeutic regimens. In the context of immunotherapy, peptide-based photosensitive nanodrugs represent promising platforms for incorporating emerging strategies such as neoantigen-based cancer vaccines and enhancing immune checkpoint blockade through co-delivery approaches or tumor-specific immune activation.; (iv) real-time monitoring and theranostics: future systems should incorporate real-time imaging and feedback mechanisms, enabling spatiotemporal control over therapy and real-time evaluation of treatment efficacy.

In summary, peptide-based self-assembly offers a flexible and robust foundation for the development of innovative photodynamic nanodrugs. Continued interdisciplinary collaboration across chemistry, nanotechnology, and biomedicine will be vital to overcoming current barriers and translating these advanced systems into clinically viable solutions for cancer therapy.

## Author contributions

Conceptualization: S. L., X. Y.; writing – original draft: S. L.; writing – review & editing: J. van H., R. X., X. Y.; supervision: X. Y.

## Conflicts of interest

There are no conflicts to declare.

## Data availability

No primary research results, software or code have been included and no new data were generated or analysed as part of this review.

## Acknowledgements

The authors acknowledge support from the National Key R&D Program of China (2023YFA0915300 and 2023YFA0915304), National Natural Science Foundation of China (no. 22207109, 22377127, and 22302207), the Beijing Nova Program (no. 20230484352 and 20240484650) and IPE Project for Frontier Basic Research (grant no. QYJC-2023-05) as well as the MSCA Postdoctoral Fellowships 2022 (no. 101104725).

## References

- 1 X. Li, J. F. Lovell, J. Yoon and X. Chen, *Nat. Rev. Clin. Oncol.*, 2020, **17**, 657–674.
- 2 L. M. Ailioaie, C. Ailioaie and G. Litscher, *Int. J. Mol. Sci.*, 2025, **26**, 2969.
- 3 J. Kelly and M. Snell, *J. Urol.*, 1976, **115**, 150–151.
- 4 D. Aebisher, K. Rogóž, A. Myśliwiec, K. Dynarowicz, R. Wiench, G. Cieślak, A. Kawczyk-Krupka and D. Bartusik-Aebisher, *Front. Oncol.*, 2024, **14**, 1373263.
- 5 X. Li, S. Lee and J. Yoon, *Chem. Soc. Rev.*, 2018, **47**, 1174–1188.
- 6 M. Abbas, Q. Zou, S. Li and X. Yan, *Adv. Mater.*, 2017, **29**, 1605021.
- 7 S. Li, Y. Li, G. Shen, J. Sun, L. K. E. A. Abdelmohsen, X. Yan and J. C. M. van Hest, *ACS Nano*, 2025, **19**, 2799–2808.
- 8 C. Yuan, W. Fan, P. Zhou, R. Xing, S. Cao and X. Yan, *Nat. Nanotechnol.*, 2024, **19**, 1840–1848.
- 9 R. Chang, C. Yuan, P. Zhou, R. Xing and X. Yan, *Acc. Chem. Res.*, 2024, **57**, 289–301.
- 10 H. Jia, J. Liu, M. Shi, M. Abbas, R. Xing and X. Yan, *Smart Mol.*, 2025, e20240067.
- 11 S. Li, R. Xing, R. Chang, Q. Zou and X. Yan, *Curr. Opin. Colloid Interface Sci.*, 2018, **35**, 17–25.
- 12 S. Li, W. Zhang, R. Xing, C. Yuan, H. Xue and X. Yan, *Adv. Mater.*, 2021, **33**, 2103733.
- 13 R. Chang, L. Zhao, R. Xing, J. Li and X. Yan, *Chem. Soc. Rev.*, 2023, **52**, 2688–2712.
- 14 S. Li, R. Xing, J. C. M. van Hest and X. Yan, *Expert Opin. Drug Delivery*, 2022, **19**, 847–860.
- 15 Y. Li, S. Li, J. F. Scheerstra, T. Patiño, J. C. M. van Hest and L. K. E. A. Abdelmohsen, *Acc. Mater. Res.*, 2024, **5**, 1048–1058.
- 16 F. Sheehan, D. Sementa, A. Jain, M. Kumar, M. Tayarani-Najjaran, D. Kroiss and R. V. Uljijn, *Chem. Rev.*, 2021, **121**, 13869–13914.
- 17 S. Kim, Y. H. No, R. Sluyter, K. Konstantinov, Y. H. Kim and J. H. Kim, *Coord. Chem. Rev.*, 2024, **500**, 215530.
- 18 Z. Liu, Y. Tang, Y. Chen, Z. Lu and Z. Rui, *Chem. Eng. J.*, 2024, **497**, 154710.
- 19 K. Liu, R. Xing, Q. Zou, G. Ma, H. Möhwalld and X. Yan, *Angew. Chem., Int. Ed.*, 2016, **55**, 3036–3039.
- 20 Z. Li, S. Li, Y. Guo, C. Yuan, X. Yan and K. S. Schanze, *ACS Nano*, 2021, **15**, 4979–4988.



- 21 S. Li, Q. Zou, Y. Li, C. Yuan, R. Xing and X. Yan, *J. Am. Chem. Soc.*, 2018, **140**, 10794–10802.
- 22 Q. Zou, M. Abbas, L. Zhao, S. Li, G. Shen and X. Yan, *J. Am. Chem. Soc.*, 2017, **139**, 1921–1927.
- 23 S. Li, L. Zhao, R. Chang, R. Xing and X. Yan, *Chem. – Eur. J.*, 2019, **25**, 13429–13435.
- 24 L. Y. Zhao, Y. M. Liu, R. R. Xing and X. H. Yan, *Angew. Chem., Int. Ed.*, 2020, **59**, 3793–3801.
- 25 R. Chang, E. Nikoloudakis, Q. L. Zou, A. Mittraki, A. G. Coutsolelos and X. H. Yan, *ACS Appl. Bio Mater.*, 2020, **3**, 2–9.
- 26 G. Z. Shen, R. R. Xing, N. Zhang, C. J. Chen, G. H. Ma and X. H. Yan, *ACS Nano*, 2016, **10**, 5720–5729.
- 27 X. Guan, B. Zhang, Z. Wang, Q. Han, M. An, M. Ueda and Y. Ito, *J. Mater. Chem. B*, 2023, **11**, 4619–4660.
- 28 Y. Liu, K. Ma, T. Jiao, R. Xing, G. Shen and X. Yan, *Sci. Rep.*, 2017, **7**, 42978.
- 29 Y. Liu, R. Xing, J. Li and X. Yan, *iScience*, 2023, **26**, 105789.
- 30 Y. Jia, X. Yan and J. Li, *Angew. Chem., Int. Ed.*, 2022, **61**, e202204709.
- 31 K. Ma, R. R. Xing, T. F. Jiao, G. Z. Shen, C. J. Chen, J. B. Li and X. H. Yan, *ACS Appl. Mater. Interfaces*, 2016, **8**, 30759–30767.
- 32 J. Li, A. Wang, P. Ren, X. Yan and S. Bai, *Chem. Commun.*, 2019, **55**, 3191–3194.
- 33 S. Li, Y. Li, M. Shi, R. Xing, J. C. M. van Hest and X. Yan, *J. Mater. Chem. B*, 2024, **12**, 10915–10922.
- 34 R. Xing, Q. Zou, C. Yuan, L. Zhao, R. Chang and X. Yan, *Adv. Mater.*, 2019, **31**, 1900822.
- 35 X. Ma, Y. Liu, S. Li, K. Ogino, R. Xing and X. Yan, *Supramol. Mater.*, 2022, **1**, 100003.
- 36 H. Javid, M. A. Oryani, N. Rezagholinejad, A. Esparham, M. Tajaldini and M. Karimi-Shahri, *Cancer Med.*, 2024, **13**, e6800.
- 37 S. Kunjiappan, P. Pavadai, S. Vellaichamy, S. R. K. Pandian, V. Ravishankar, P. Palanisamy, S. Govindaraj, G. Srinivasan, A. Premanand, M. Sankaranarayanan and P. Theivendren, *Drug Dev. Res.*, 2021, **82**, 309–340.
- 38 S. Cao, Y. Xia, J. Shao, B. Guo, Y. Dong, I. A. B. Pijpers, Z. Zhong, F. Meng, L. K. E. A. Abdelmohsen, D. S. Williams and J. C. M. van Hest, *Angew. Chem., Int. Ed.*, 2021, **60**, 17629–17637.
- 39 A. Borrelli, A. L. Tornesello, M. L. Tornesello and F. M. Buonaguro, *Molecules*, 2018, **23**, 2956.
- 40 S. K. Li, W. J. Zhang, H. D. Xue, R. R. Xing and X. H. Yan, *Chem. Sci.*, 2020, **11**, 8644–8656.
- 41 N. Zhang, F. F. Zhao, Q. L. Zou, Y. X. Li, G. H. Ma and X. H. Yan, *Small*, 2016, **12**, 5936–5943.
- 42 H. F. Sun, S. K. Li, W. Qi, R. R. Xing, Q. L. Zou and X. H. Yan, *Colloids Surf., A*, 2018, **538**, 795–801.
- 43 B. Sun, X. Guo, M. Feng, S. Cao, H. Yang, H. Wu, M. H. M. E. van Stevendaal, R. A. J. F. Oerlemans, J. Liang, Y. Ouyang and J. C. M. van Hest, *Angew. Chem., Int. Ed.*, 2022, **61**, e202202518.
- 44 B. Sun, R. Chang, S. Cao, C. Yuan, L. Zhao, H. Yang, J. Li, X. Yan and J. C. M. van Hest, *Angew. Chem., Int. Ed.*, 2020, **59**, 20582–20588.
- 45 D. H. T. Le, V. Ibrahimova, S. A. H. van den Wildenberg, H. Wu, A. Fonseca, T. Torres, E. Garanger, W. P. J. Leenders, R. Brock, S. Lecommandoux and J. C. M. van Hest, *Angew. Chem., Int. Ed.*, 2023, **62**, e202306182.
- 46 Q. Zou, R. Chang, R. Xing, C. Yuan and X. Yan, *J. Controlled Release*, 2020, **319**, 344–351.
- 47 M. Abbas, R. Xing, N. Zhang, Q. Zou and X. Yan, *ACS Biomater. Sci. Eng.*, 2017, **4**, 2046–2052.
- 48 H. Zhang, K. Liu, S. Li, X. Xin, S. Yuan, G. Ma and X. Yan, *ACS Nano*, 2018, **12**, 8266–8276.
- 49 R. Xing, K. Liu, T. Jiao, N. Zhang, K. Ma, R. Zhang, Q. Zou, G. Ma and X. Yan, *Adv. Mater.*, 2016, **28**, 3669–3676.
- 50 C. Wang, Y. Xiu, Y. Zhang, Y. Wang, J. Xu, W. Yu and D. Xing, *Nanoscale*, 2025, **17**, 1812–1873.
- 51 Y. X. Li, R. C. H. Wong, X. H. Yan, D. K. P. Ng and P. C. Lo, *ACS Appl. Bio Mater.*, 2020, **3**, 5463–5473.
- 52 B. Sun, H. Yang, Y. Li, J. F. Scheerstra, M. H. M. E. van Stevendaal, S. Li and J. C. M. van Hest, *Biomacromolecules*, 2024, **25**, 3044–3054.
- 53 Y. Li, P. Sun, L. Zhao, X. Yan, D. K. P. Ng and P. C. Lo, *Angew. Chem., Int. Ed.*, 2020, **59**, 23228–23238.

